Nonlinear Electromagnetic Systems
A.J. Moses and A. Basak (Eds.)
IOS Press, 1996

INTEGRO-DIFFERENTIAL METHOD FOR PERMANENT MAGNET MODELING IN 3-D SPACE USING EDGE FINITE ELEMENTS

Vlatko Čingoski and Hideo Yamashita
Hiroshima University, Kagamiyama 1-4-1, Higashi-hiroshima 739, JAPAN

Abstract. In this paper, an integro-differential method for the modeling of permanent magnets in 3-D space using edge finite elements is presented. The value of the coercive magnetic force $\mathbf{H}_c$ is integrated over the entire permanent magnet surface area. This procedure results in direct computation of the equivalent source current $\mathbf{I}_{pm}$, which is afterwards assigned to surface edges of the permanent magnet. The proposed method exhibits accurate results with less computation effort and an improved convergence rate of the iterative solver. Also, presented in this paper is a comparison of the results for a simple test model obtained by the integro-differential method and those obtained by the Biot-Savart Law and the current-sheet method. A comparison between numerical results and measured results for more complicated application model is also given.

1. Introduction

The use of permanent magnets (PMs) in electrical devices has greatly increased in recent years. Furthermore, new materials like ceramic magnets have appeared on the scene and are commonly available at a relatively low price. It is becoming increasingly important, therefore to accurately compute the magnetic field phenomena of PMs.

Due to the existence of a non-explicit field source, the computation of magnetic field phenomena of PM depends on the modeling method used. The easiest and most widely employed method for modeling PM devices is the current-sheet method, which however, has a major disadvantage: it is applicable for only simple geometrical PM shapes. Improvements of this method in order to model more complicated PM shapes have been investigated, but unfortunately, only after many approximations and much effort [1], [2].

Mainly because of its computational advantages, the FEM based on edge finite elements has recently become widely employed. On the other hand, the problem of satisfaction of the solenoidal character of the source current using edge finite elements and the current-sheet method is strongly emphasized, especially for complicated shapes of PMs and ultra-thin sheet conductors, resulting in a large number of iterations and long computation time.

In this paper, the authors present an integro-differential method for 3-D modeling of PM using edge finite elements. This method, which was previously proposed for nodal FEA [3], is extended and applied on edge finite elements. Due to the different nature of nodal and edge finite elements, a new mathematical model for computing the equivalent source current intensity vector was developed. The method is easy applicable to any PM shape and exhibits improvement of the convergence rate of the iterative solver with highly accurate results.

2. Integro-differential Method and Its Numerical Implementation

The rationale for the integro-differential method for modeling of PMs using nodal finite elements has been already introduced [3]. Therefore, here we will only address a number of peculiarities which arise from the edge finite element implementation of this method.

2.1. Mathematical Background

In nodal FEA the generated finite element mesh is node oriented. In edge FEA, on the other hand, the developed mesh must be edge oriented. This means that the basic computation "cell" is an edge of the mesh not a node. In addition, the unknown variables, boundary conditions and source vectors have to be assigned directly to edges of the mesh, not to the nodes.

This conclusion is also valid for the source current values, which in edge FEA can be assigned directly to mesh edges as source current intensity values, or indirectly by means of the current vector potential [4]. Using the current-sheet method, only simple PM shapes can be modeled. Another problem is satisfaction of the solenoidal character of the source current which can be strongly emphasized in case of ultra-thin conductors and complicated PM shapes. Use of ultra-thin conductors in the current-sheet method is imperative, however, if an accurate analysis is called for. Decreasing the thickness of the current-sheet towards zero results in increasing the accuracy of the results. Theoretically, for conductor thickness equal to zero, an approximation will be the best. This is impossible for the current-sheet method, however, as area carrying current degenerates toward zero. As we can see further, this is possible using the integro-differential method over a mesh of edge based finite elements.

Typical working demagnetization curve of PM can be expressed with the following equation

$$\mathbf{H} = \nu(\mathbf{B})\,\mathbf{B} - \mathbf{H}_c\,, \tag{1}$$

where ν is the reluctivity coefficient, and $\mathbf{H}_c$ is the coercivity. Substituting (1) in the Ampere's Law we obtain the following equation

$$\nabla \times \nu(\mathbf{B})\,\mathbf{B} \;=\; \mathbf{J}_0 \;+ \nabla \times \mathbf{H}_c\,. \tag{2}$$

In case of a linear magnetic circuit, the reluctivity coefficient ν has to be computed only once by the following equation

$$\nu \;=\; \frac{\mathbf{H}_c}{\mathbf{B}_r}\,, \tag{3}$$

where $\mathbf{B}_r$ is the residual magnetization. For nonlinear magnetic circuits, however, the demagnetization curve must be shifted to the right equal to the amount of the coercivity $\mathbf{H}_c$, and the reluctivity coefficient must be recomputed at each nonlinear step as

$$\nu(\mathbf{B}) = \frac{\mathbf{H} \,+\, \mathbf{H}_c}{\mathbf{B}}\,. \tag{4}$$

In (2), the second term on the left side, $\nabla \times \mathbf{H}_c$, is the equivalent current density value of the permanent magnet $\mathbf{J}_{pm}$, whose numerical implementation we will briefly describe in the next paragraph.

2.2. Numerical Implementation

Using magnetic vector potential formulation and applying the Galerkin Method with vectorial shape functions $\mathbf{N}_i$ as a trial functions, the governing equation for magnetostatic problems without source current has the following configuration

$$\int_V \mathbf{N}_i[\nabla \times (\nu\nabla \times \mathbf{A})]\, dV = \int_V \mathbf{N}_i\, (\nabla \times \mathbf{H}_c)\, dV\,, \tag{5}$$

where V is the total volume of the analyzed region. Applying the Stokes' Theorem on the left hand side of (5) we obtain

$$\int_V \nabla \times \mathbf{H}_c\, dV \;=\; \int_S \mathbf{H}_c \cdot d\mathbf{S}\,, \tag{6}$$

where $d\mathbf{S}$ is the vectorial surface area of each finite element. This procedure must be performed for each finite element "inside" the PM area. Since the outward normals of two adjoining surfaces always have opposite directions, the integral for each surface that lies "inside" PM is canceled. Therefore, the integration is reduced only on the surface area of the PM. Rewriting (6) as

$$\int_S \mathbf{H}_c \cdot d\mathbf{S} \;=\; \mathbf{H}_c \times \mathbf{S}\,, \tag{7}$$

where $\mathbf{S}$ is the vector with intensity S equal to the triangular surface area of each finite element lying on the PM surface and with the same direction as the outward normal on that surface, another important conclusion emerges. That is, all surfaces which have the outward normal collinear with the direction of the coercivity vector $\mathbf{H}_c$ must be excluded from the analysis, reducing the computational region. Finally, using (7) we can compute the intensity

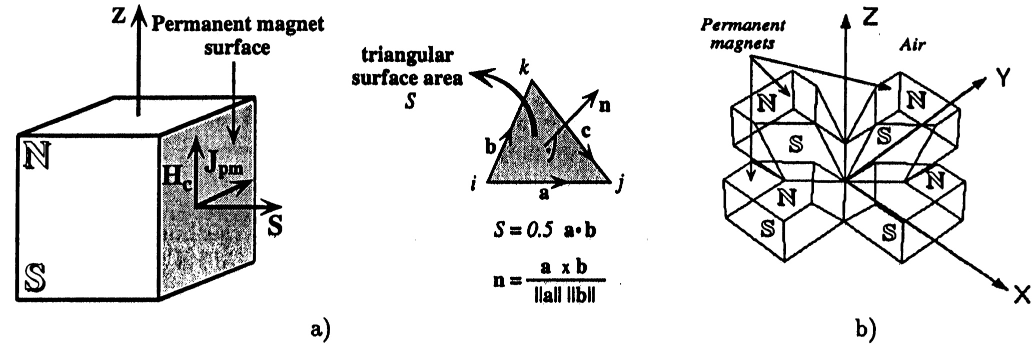

Fig. 1. Analyzed models
a) simple test model with definition of the equivalent source current $\mathbf{J}_{pm}$, normal vector $\mathbf{n}$ and triangular surface area S b) application model

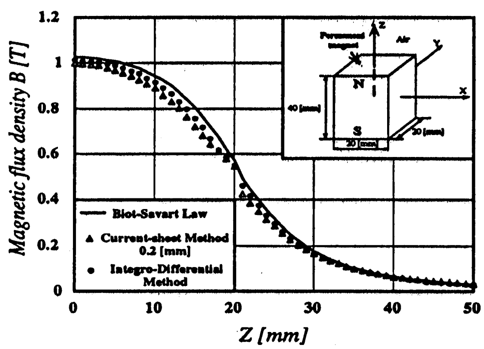

Fig. 2. Comparison of results

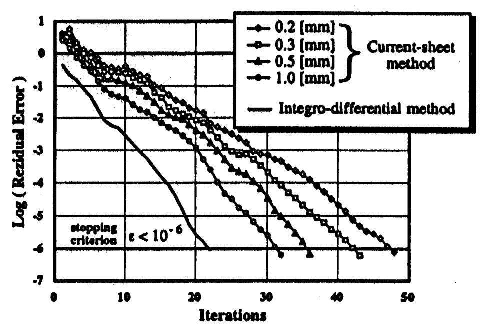

Fig. 3. Convergence rate

and direction of the equivalent source current vector $\mathbf{I}_e$ defined by the vector product (7) (see Fig. 1a) using the following equation:

$$\mathbf{I}_e = \frac{(\mathbf{H}_c \times \mathbf{n})\, S}{l_e}\,. \tag{8}$$

Afterwards, vector $\mathbf{I}_e$ must be assigned to surface edge e with length l_e. The triangular surface area S and its normal vector $\mathbf{n}$ can easily be computed using two of its three edges as shown in Fig. 1a.

3. Simple Test Model

A simple test model was constructed (see Fig. 1a) of a rectangular PM with dimensions $20\,[mm] \times 20\,[mm] \times 40\,[mm]$, relative permeability $\nu_r = 1.07$ and coercivity $\mathbf{H}_c = \{0, 0, H_{cz}\} = \{0, 0, 870000\}\ [A/m]$. The model was analyzed using the proposed integro-differential method, the current-sheet method and the Biot-Savart Law. In case of the current-sheet method, four different current sheets were developed with thicknesses: 0.2 $[mm]$, 0.3 $[mm]$, 0.5 $[mm]$ and 1.0 $[mm]$. The obtained results for the z-component of magnetic flux density vector $\mathbf{B}$ along central axis of the model – vertical line $z = 0\ [mm] \sim 50\ [mm]$ are presented in Fig. 2. From Fig. 2 it is clear that the accuracy of the proposed method is greater than that of the current-sheet method. In addition, the proposed method exhibits improvements in the convergence rate. This can be understood from the results given in Table 1 and Fig. 3. From Fig. 3 it is apparent that the proposed method requires fewer numbers of iterations for the same residual. In case of the current sheet method, the number of iterations is inversely proportional to the current-sheet thickness.

4. Application

After numerical verification of the accuracy of the integro-differential method was carried out

TABLE 1. *Integro-differential method vs. current sheet method and Biot-Savart Law*

	Current-sheet Method [*mm*]				Biot-Savart Law	Integro-differential Method
	0.2	0.3	0.5	1.0		
B_{max} [*T*]	1.012	1.010	1.003	0.999	1.025	1.020
Number of iterations	48	43	36	32	/	22

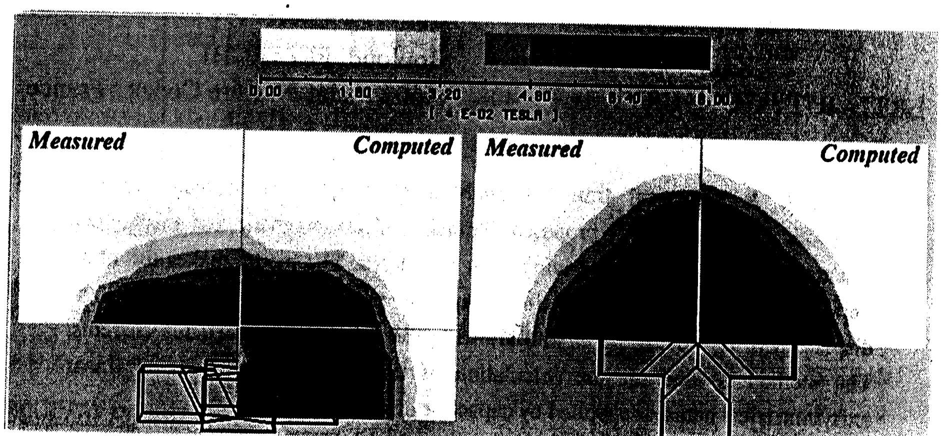

a) side view b) top view

Fig. 4. Comparison between measured and computed results

using a simple test model, the proposed method was applied for analysis of the magnetic field distribution of the 3-D model presented in Fig. 1*b*. This model is constructed of four symmetrical PM with rather complicated shapes. Only 1/4 of the model was analyzed using the proposed integro-differential method. Due to the complexity of the model, the Biot-Savart Law was not applicable for verification of the results. For this model, however, the measured results were available. In Fig. 4, a comparison between the 3-D magnetic flux density distributions obtained by the proposed method and those obtained by the measurements is presented. From Fig. 4, it is clear that the results are nearly equivalent.

5. Conclusions

We presented an integro-differential method for the modeling of permanent magnets in 3-D space using edge finite elements. The proposed method exhibits such improvements over the conventional current-sheet method as: computational efficiency and accuracy, and easy modeling of arbitrary 3-D PM shapes. It is applicable for linear and nonlinear magnetic circuits. The results obtained with the proposed method are in very good agreement with the measurements and with the results obtained by the Biot-Savart Law.

References

[1] F. A. Fouad, T. W. Nehl and N. A. Demerdash *Permanent magnet modeling for use in vector potential finite element analysis in electrical machinery*, IEEE Trans. on Magn., Vol. Mag-17, No. 6, November 1981, pp.3002-3004.

[2] J. R. Brauer, L. A, Larkin and V. D. Overbye *Finite element modeling of permanent magnet devices*, J. Appl. Phys., 55(6), 15 March 1984, pp.2183-2185.

[3] R. H. Vander Heiden, J. R. Brauer, J. J. Ruehl and G. A. Zimmerlee *Utilizing permanent magnets in nonlinear three-dimensional finite element models*, IEEE Trans. on Magn., Vol. 24, No. 6, November 1988, pp.2931-2933.

[4] V. Čingoski, K. Kaneda and H. Yamashita *On the current input in 3D finite element analysis using tetrahedral edge finite element*, International Journal of Applied Electromagnetics in Materials, Vol. 3, 1994, pp.357-367.